Conference Proceedings

Solar World Congress 2015
Daegu, Korea, 08 – 12 November 2015

NUMERICAL INVESTIGATION OF SOLAR PARABOLIC TROUGH RECEIVER UNDER NON UNIFORM SOLAR FLUX DISTRIBUTION

C. Ananthsornaraj [1] and K. S. Reddy[2]

[1] Research Scholar, Heat Transfer and Thermal Power Laboratory, Department of Mechanical Engineering, Indian Institute of Technology Madras, Chennai-600036, INDIA

[2] Professor, Heat Transfer and Thermal Power Laboratory, Department of Mechanical Engineering, Indian Institute of Technology Madras, Chennai-600036, INDIA

Abstract

Three dimensional numerical modeling of parabolic trough receiver is performed to study the non uniform flux distribution on the outer surface of the receiver by coupling Monte Carlo Ray-Tracing Method (MCRT) with the Finite Volume Method (FVM) and calculated non uniform flux distribution is considered as a thermal boundary condition. The numerical model is solved by considering RNG k–ε turbulent model. In this paper, different Heat Transfer Fluids (HTF) with respect to the various operating parameters such as mass flow rate, Direct Normal Irradiation (DNI), inlet temperature and ambient conditions are considered. The temperature profile of both absorber and glass envelope follows the non-uniform solar heat flux distribution curve. Three dimensional temperature distribution of the absorber tube is calculated numerically for different inlet temperature and velocity of HTF. The maximum solar heat flux attained by the PTC receiver is 9753.3 W/m^2, 19506 W/m^2, 29260 W/m^2, and 39013 W/m^2 when the DNI are 200 W/m^2, 400 W/m^2, 600 W/m^2, and 800 W/m^2 respectively.

Keywords: *Solar Energy; Parabolic Trough Collector; Non uniform flux distribution; Computational Fluid Dynamics*

1. Introduction

Parabolic Trough Collector (PTC) system is having considerable attention among the other solar concentrators because it needs only single axis tracking and moderate receiver operating temperature. The receiver is the key element of the PTC system where solar radiation is absorbed and converted into thermal energy (Kalogirou, 2004). The receiver is placed on the focal line and it heats the Heat Transfer Fluid (HTF) which flows through it. The incident solar radiation which falls on the collector eventually gets concentrated on the receiver surface which gets converted into thermal energy. The heat transfer process of receiver can be summarized as: the incident solar radiation on the absorber, the convection heat transfer between the HTF and the absorber, the conduction and radiation heat transfer through the absorber wall and the glass tube, and the heat transfer from the glass tube to the ambient (Mahoney, 2002). Non uniform flux developed on the outer surface of receiver due to the concentration of solar energy results in thermal stress and circumferential temperature difference on the absorber wall are the prime reason for the failure of PTC receiver tube. The temperature increase depends on the geometrical concentration ratio and optical properties of the collector as well as fluid flow in the absorber tube. Accurate studies are needed to find three dimensional temperature distributions of the absorber tube and its thermal expansion and deformation for any safe and efficient operation. Deformation of the absorber tube takes place due to a non-uniform thermal expansion (Iverson et al., 2011). Due to this deformation of PTC receiver, it will go out of focal point and causes different problems such as decreasing the life time of collector, breakage of cover glass tube and also it drops optical efficiency of the collector. Edenburn et al., (1976) predicted the efficiency of a PTC by using an analytical heat transfer model for evacuated and non-evacuated cases. The results showed good agreement with

doi:10.18086/swc.2015.04.08 Available at http://proceedings.ises.org

measured data obtained from SNL collector test facility (Pope et al., 1973). Ratzel et al., (1979) carried out both analytical and numerical study of the heat conduction and convective losses in an annular receiver for different geometries. Three techniques were proposed to reduce the conduction heat loss: evacuation, over sizing the annular receiver while keeping the Rayleigh number below 1000 over the range of operation and use of gases with low thermal conductivity. Clark (1982) analyzed the effects of design and manufacturing parameters that influenced the thermal and economical performance of parabolic trough receivers

Recently, Cheng et al., (2012) reported a three-dimensional simulation of a parabolic trough solar collector with non-uniform solar flux conditions by incorporating the FVM and the MCRT method, in which the effects of the properties of different HTFs to the whole temperature distributions in the receiver, the thermal loss and the collector efficiency were numerically studied Moreover, the effects of the DNI, Reynolds number and emissivity of the inner tube wall on the outlet temperature, average temperature of absorber outer wall, thermal radiation loss and efficiency, and the concentrating characteristics of the parabolic trough solar collectors PTC (He et al., 2011) were discussed. Because of the non-uniform distributions of the solar energy flux, there exist CTD of the absorber and the cover, which has a crucial influence on the circumferential stress and the deformation of the receiver tubes. Numerous studies have been carried out to investigate the temperature distributions and thermal stress fields of tubes and receivers with various material conditions. A numerical analysis had been conducted by Chen et al., (2004) to study the effect of using porous material for the receiver on temperature distributions. Experiments were conducted by Fend et al., (2004) to research the temperature distributions on the volumetric receivers used two novel porous materials. Numerical simulations are used to investigate the detailed temperature distribution, and its corresponding structural deformation of the stainless steel tube of PTR. The simulations are performed by combining a MCRT code and Finite Volume Method. The non-uniform concentrated solar heat flux on the steel pipe was obtained through the MCRT method (He et al., 2011). The fluid–solid coupled heat transfer was solved with the finite volume method. The concentrated solar heat flux was used as a boundary condition of the fluid–solid coupled heat transfer modeling. In the annular vacuum gap, the conduction was ignored, and the infrared radiation heat transfer was treated as a gray enclosure and modeled with S2S radiation model. In the CFD simulations, the studied PTR (Fig. 1) was assumed to be structurally rigid, and its surfaces have wavelength independent properties. The HTF (heat transfer fluid) had temperature dependent properties. Güven et al., (1986) established an optical model which used a ray-tracing technique to evaluate the optical performance and determined the optical errors by means of a statistical analysis. Valladares et al., (2009) proposed a numerical simulation of the optical, thermal and fluid dynamic behavior of a single-pass solar PTC and extended the study by replacing the absorber with counter-flow concentric circular heat exchangers (double-pass). Kumar et al., (2009) investigated heat transfer enhancement of solar receivers with porous insertions by numerical simulation and found that significant heat transfer improvement (64.3%) was obtained. Stuetzle et al., (2002) proposed a 2D unsteady state analysis of solar collector absorber to calculate the collector field outlet temperature: the model was solved by discretizing the partial differential equations obtained by the energy balance.

2. Description & Specification of PTC System

The parabolic solar collector tube consists of cylinder. The inner tube is a metallic tube and the outer tube is a glass tube. Fig. 1 shows the physical geometry and cross section of PTC, which is made by bending a sheet of reflective material into a parabolic shape surface. A receiver tube is placed along the focal line of the parabolic reflective collector. The receiver tube usually includes an inner absorber tube and a glass cover. The glass cover is used for reducing heat loss; as well as the annular space between the inner tube and the glass cover is vacuumed, which helps to decrease the convection heat loss. Fig.1, should include the following processes: convection heat transfer between the HTF and the absorber; solar irradiation absorption in the absorber; conduction heat transfer through the absorber wall; heat transfer from the absorber to the glass tube; solar irradiation absorption in the glass tube; conduction heat transfer through the glass tube; heat transfer from the glass tube to the atmosphere, etc. Particularly, both the convection and the radiation heat transfer occur between the outer absorber surface and the inner glass tube surface. The convection heat transfer mechanism depends on the annulus pressure (KJC Operating Company, 1993). It may either be

molecular conduction or free convection. The heat transfer from the glass tube to the atmosphere is also caused by convection and radiation, where the convection is either forced or natural, depending on whether there is wind around the glass tube.

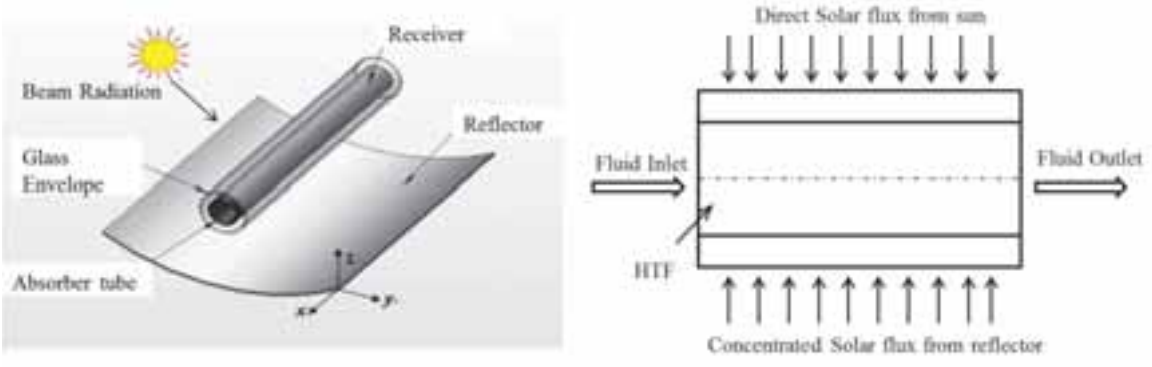

(a) (b)

Fig. 1: Physical model (a) Schematic of PTC (b) Cross section view

The radiation heat transfer occurs due to the temperature difference between the outer absorber surface and the inner glass tube surface, so does the glass tube and sky.

3. Numerical modeling and analysis

The simulations consist of Monte-Carlo ray tracing, CFD modeling. Firstly, Monte-Carlo ray tracing was used to calculate the concentrated solar radiation heat flux distribution on the stainless steel tube (absorber tube) of PTR. This flux distribution is treated as a boundary condition of the CFD analysis. Secondly, CFD was used to model the flow and heat transfer (including convection, conduction and radiation heat transfer) in the PTC receiver.

3.1 Governing Equation

The geometrical model of PTC receiver is shown in Fig.1. The heat transfer process in PTC can be summarized as: the incident solar radiation on the absorber, convection heat transfer between HTF and absorber, conduction and radiation heat transfer through the absorber wall and the glass tube, and heat transfer from the glass tube to the ambient.

As the test conditions shown in Table 1, the fluid flow is in turbulent and in steady state conditions. So the governing equations is given by (Cheng et al., 2010)

$$\partial/\partial x_i(\rho u_i) = 0 \qquad \text{(eq. 1)}$$

$$\rho C_p u_i \frac{\partial T}{\partial x_i} = (k + k_i)\frac{\partial}{\partial x_i}\left(\frac{\partial T}{\partial x_i}\right) \qquad \text{(eq. 2)}$$

$$\frac{\partial T}{\partial x_j}\left(\rho u_i u_j\right) = -\frac{\partial P}{\partial x_i} + \frac{\partial}{\partial x_j}\left[\ (\mu + \mu_i)\left(\frac{\partial u_i}{\partial x_j} + \frac{\partial u_j}{\partial x_i}\right) - \frac{2}{3}(\mu + \mu_i)\frac{\partial u_i}{\partial x_i}\delta_{ij} - \frac{2}{3}\rho k\delta_{ij}\right] + F \qquad \text{(eq. 3)}$$

3.2 Boundary conditions

The boundary conditions used in this study are:

(1) For the fluid domain, the inlet boundary conditions are defined as the mass flow rate and inlet temperature of HTF. Similarly the outlet boundary condition is fully developed flow condition. Adiabatic boundary condition is applied at both the ends of the receiver walls (Thermal insulation at the absorber end).

Inlet: $m = m_{in}$, $T = T_{inlet}$ $kin = 0.005\rho u_x^2$, $\varepsilon_{in} = C\mu\, \rho_f\, k_{in}^2 / \mu_t$

Where $C\mu = 0.09$, $\mu_t = 100$

Outlet: Fully developed flow condition

(2) Periodic boundary conditions are used for the absorber tube's inlet and outlet. The inner absorber tube walls are considered no-slip and no-penetration .The outer wall of the absorber tube receives a non uniform heat flux. The lower half receives almost concentrated solar radiation while the upper half receives direct solar radiation

(3) The inner surface of absorber tube and the heat transfer fluid were defined as coupled fluid–solid interfaces in which the energy is conserved.

(4) The outer surface of absorber tube and inner surface of glass envelope are formulated by the surface-to-surface radiation

(5) The outer surface of the glass envelope was defined with a mixed boundary with convection and radiation.

(a) Convection boundary condition: (i) if the convection was assumed to be natural (no wind around the PTC receiver) the correlation to estimate heat transfer coefficient .

$$h = {Nu_{D,g}\lambda}\Big/{D_{g,o}} = {\left(\left(0.48\, Ra_{D,go}{}^{0.25}\right)\lambda\right)}\Big/{D_{g,o}} \qquad \text{(eq. 4)}$$

(ii) if the convection was assumed to be forced (presence of wind around the PTC receiver) the experimental correlation to calculate the heat transfer coefficient (Mullick and Nanda, 1989)

$$h = 4V_w{}^{0.58} D_{g,o}{}^{-0.42} \qquad \text{(eq. 5)}$$

(b) Radiative boundary condition**:** The Stefan– Boltzmann law is used to calculate the net radiation transfer by assuming that the glass cover is a small convex gray object in a large blackbody cavity (sky, approximated 8℃ below the ambient temperature). i.e. surface to ambient condition

(6) For the inlet and outlet of the receiver's annulus space, symmetry boundary condition is used such that the normal gradients of all flow variables are zero.

3.3 Computational domain and Properties of HTF:

The computational domain includes the absorber tube domain (solid), the liquid oil domain (fluid) . The material for the solid domain is stainless steel and the thermal conductivity is fixed at 54 W /m.K. Syltherm 800 liquid oil was used as the working fluid. And the properties of working fluid, such as: isobaric specific heat capacity (cp), thermal conductivity (l), density (r) and dynamic viscosity (m) should be selected to simulate the heat transfer process in absorber tube by FLUENT. The properties of HTF are considered to be temperature dependent (He et al., 2011).

3.4 Grid independent study

To guarantee that the computed results were accurate and reliable, a grid independence study was conducted. Simulations with three grids (50,000, 60,000, 70,000, 80,000 elements) were performed. Four different grids are chosen to calculate the temperature difference between the inlet and outlet of PTC receiver for the same boundary conditions. There are less than 2% differences temperature increment between grid 3

and grid 4. The authors concluded that 80,000 elements are enough for this study, and grid 4 with 80,000 elements was used all over this study. It is a traditional grid independence test method for the fluid and heat transfer problem. It should be noted that the minimum grid density is limited by the systematic error.

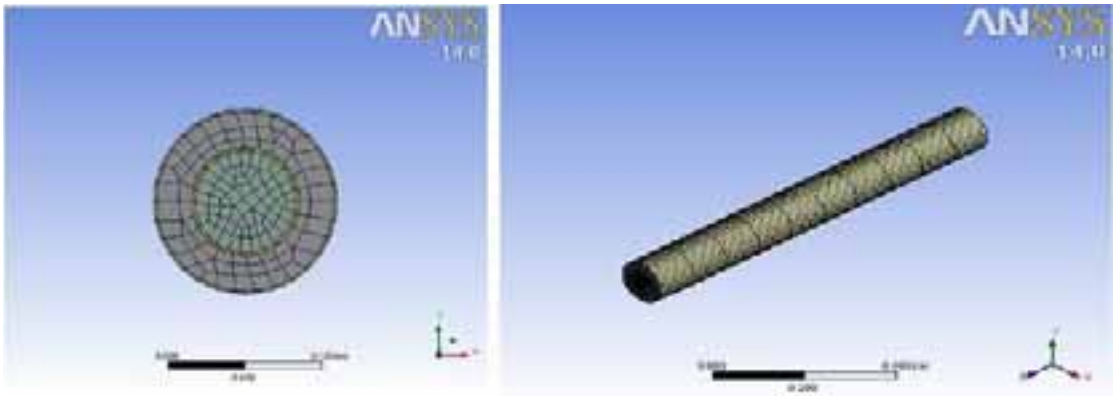

Fig. 2: Grid generated view of fluid region, absorber and glass envelope

4. Numerical modeling and Analysis

A three dimensional mesh was generated and used in this study, see Fig. 6. Dense grids were generated near the bellows where large temperature gradient exists. This three dimensional conjugate heat transfer problem was solved using the CFD software Ansys 14. The standard k–e model (high Reynolds number) was used along with conventional wall functions in this study. The SIMPLE algorithm was used to couple the pressure and the velocities with the second order upwind method used for the advection terms in the momentum equations and for the energy equation. User defined functions (UDF) were used to define the concentrated solar radiation flux on the selective coating and the circumferential distributed source term of the glass envelop. The used discretizations of all the solved equations were second order. The convergence criterion was set to 10^{-4} for continuity and momentum equations and 10^{-7} for energy equation. Radiative heat loss from the receiver pipe solely depends on the emissivity of the pipe, temperature of the pipe and the temperature of the surrounding objects. Hence the receiver pipe and the glass envelope were assumed to be gray and diffuse, and were simulated by surface-to-surface (S2S) radiation model. The glass envelope is assumed to be opaque to the radiation within the infrared energy spectrum.

.4.1 Monte Carlo Ray Tracing (MCRT) Method

The flowchart of the Monte Carlo Ray-Trace method for the photon energy concentrating and collecting process of the whole PTC system is shown. The reflection Ray vector Rs is expressed according to the Fresnel law. Once the photon packet is initialized, the photon is moved, traced in the PTC system, and judged if it hits a boundary (surface) of one of the subsystems or components (such as the glass tube, the reflector and the absorber) on the way of the photon propagated where it may be reflected, absorbed or transmitted. The photon is repeatedly moved until it either escapes from or is absorbed by the system. If the photon hits a boundary when propagating, the corresponding judgment of reflecting, absorbing or transmitting event is adopted by the Monte Carlo method. If the photon escapes from the system, the corresponding parameter of recording the escaped photons is updated. If the photon is absorbed, the position of the absorption and the absorbed energy weight are recorded. This process is repeated until the desired numbers of photons have been propagated. Then the code validations are made and the non-uniform solar energy flux distribution is calculated.

4.2 Combine MCRT Method with FVM

The solar energy flux distribution on the outer wall of the inner absorber tube calculated by in-house developed Monte Carlo Ray- Trace (MCRT) code, then this flux is treated as the heat flux boundary for the simulation model in the FLUENT software with a self developed subroutine program. The self-developed

subroutine program forms a data file of the solar energy flux distribution that can be read by the FLUENT software as a boundary condition, while treating the solar absorption as a surface phenomenon.

5. Validation of Proposed Numerical Model

To further validate the reliability of the presented model, numerical simulations are simulated at the same operating conditions as Sandia test (Dudley.et al., 1994). The calculated heat flux by coupled MCRT and FVM method is validated with the existing model .The present model shows the 15% deviation with the existing developed model. Similarly the simulated circumferential temperature distribution of absorber also validated with existing model.

5.1 Validation of MCRT Code:

To validate the MCRT code, the calculation is performed on the same conventional PTSC as described .(He et al., 2011).using the MCRT method. Figure 10 shows the comparison between the circumferential local concentration ratio (LCR) distribution calculated by the MCRT method in this paper and by the semi infinite integration formulation .From that can be obviously seen that the two LCR distributions have a good agreement, which proves the MCRT code applied in the present study is accurate and reliable. Fig.2 presents the heat flux on the parabolic trough receiver surface. Numerical results show that the predicted results agree well with Wu et al., (2014), which also proves that the MCRT method used in the present study are feasible and the numerical results are reliable.

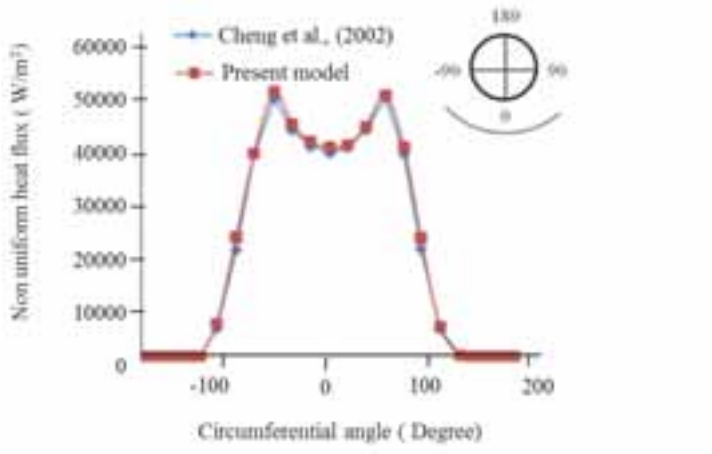

Fig. 4: Non uniform heat flux distribution around the receiver

5.2 Validation of Coupled FVM - MCRT Heat transfer Process:

To validate the simulation method for the coupled heat transfer process within the PTR, the simulation method is performed on the experimental model presented in Dudley et al (1994).

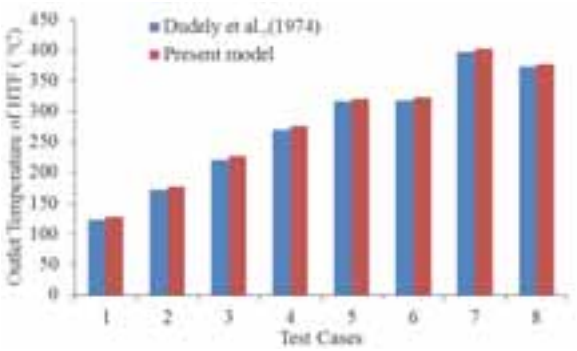

Fig. 5: Validation of receiver outlet temperature with Dudley et al., (1974)

The simulation results and the experimental data under the same conditions. The model results are validated using the data provided by the Sandia National Laboratory .It is indicated that the simulation results agree well with the experiment data, validating the accuracy of the simulation method for the coupled heat transfer process. Tests were also performed with vacuum and with air at ambient pressure in the annulus, and without the glass envelope. The measured data considering the vacuum in the annulus is given in Table 2 and the corresponding validation results are demonstrated in Figure 5. Most of the experiments were done using Syltherm 800 as the HTF, and its thermal properties .The results obtained were overall close to the measured data, with a difference of 4 to 8 ºC.

6. Results and Discussion

The developed simulated model is used to simulate the Non uniform heat flux distribution of receiver. The temperature distribution of the receiver along the length of the absorber tube as well as around the circumferential direction of the PTC receiver. The outlet temperature of HTF is calculated for the given type and mass flow rate of HTF. The simulations are carried out with vacuum condition, around 10^{-4} Torr pressure in annulus region. Due to this the convective heat losses from the absorber to the envelope are negligible, and most of the solar energy absorbed by the coating surface is transferred to the HTF. The temperature distributions of the solar receiver are crucial for the collection of the heat, which will further affect the efficiency of the collector. It is found that the inlet velocity and temperature of the HTF and the DNI will bring an important impact on the temperature distribution of the receiver, which will be numerically investigated in this section. The density, specific heat capacity, viscosity and conductivity of the fluid and the physical properties on the tube material properties are dependent on the temperature distribution of the HTF and it is also estimated from the equations. In the calculation, the velocity in the receiver tube is a parabolic form in fully developed flows. However, it should be pointed out that in real cases the distribution of the inlet velocity of the HTF in tubes presents a parabolic form. In order to simulate a real environment, applying real inlet velocity distribution is important for the improvement of the simulation results, and this issue should be further investigated in the future.

6.1 Non uniform Solar Heat Flux distribution on the outer surface of absorber

An optical model is also developed to calculate the non uniform solar flux distribution around the receiver by using MCRT method. The solar flux density distributions on the outer surface of absorber tube are illustrated in Figures 6 (a) and (b), respectively. The concentrated solar energy is mainly distributed on the bottom surface of the absorber tube.

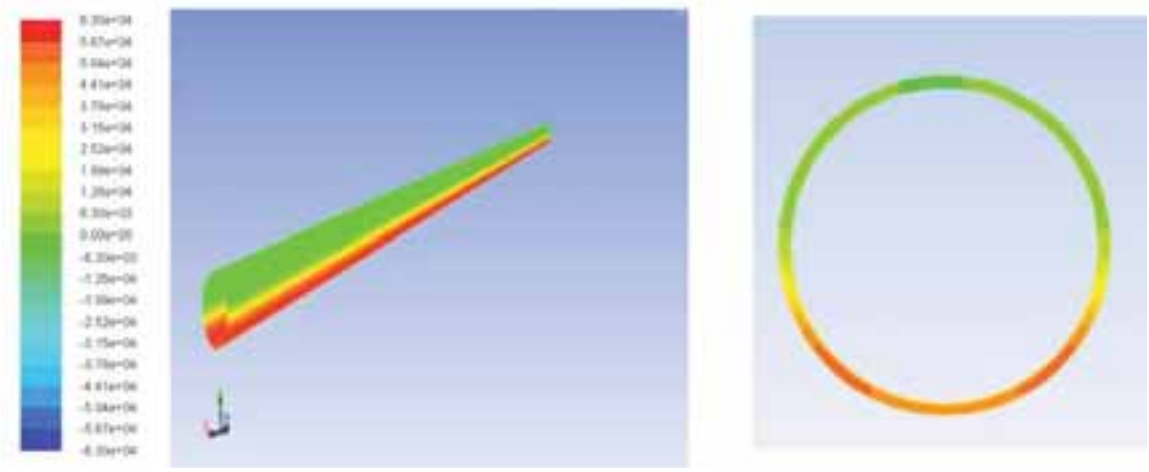

(a) (b)

Fig. 6: Non uniform flux distribution of the receiver for DNI =1000 W/m^2 (a) Axial length (b) Cross section view

The asymmetry in the two sides of the peak heat flux on the absorber is due to the presence of simulated tracking error. Because of this non uniform concentrated solar flux distribution, temperature distribution of PTC receiver in circumferential direction also non uniform. The heat flux distribution on the outer surface of absorber tube for the DNI of 800 W/m^2 and 1000 W/m^2 is shown in Figs. 6. The asymmetric distribution of heat flux in circle direction is obviously, but the heat flux distribution in axial direction (x) is uniform, as shown in Fig. 6. In order to further confirm the accuracy of the proposed MCRT code for calculating the solar energy flux distribution of the whole PTC system, numerical simulation is carried out at the same collector solar flux at about 48766 W/m^2 at the bottom portion of the absorber tube while the lowest solar flux is 1000 W/m^2 at the top portion of the absorber tube. The maximum solar heat flux attained by the PTC receiver is 9753.3 W/m^2, 19506 W/m^2, 29260 W/m^2, and 39013 W/m^2 when the DNI are 200 W/m^2, 400 W/m^2, 600 W/m^2, and 800 W/m^2 respectively.

6.2 Temperature Distribution of PTC Receiver:

Temperature distribution of PTC receiver plays the important role to determine the thermal efficiency and heat loss of PTC. The temperature contours at the absorber outlet with different inlet temperature of HTF for the DNI = 1000 W/m^2 and Inlet velocity = 1 m/s are shown in the Figure.7. The inlet temperature of HTF is high, the outlet temperature of absorber increased significantly.

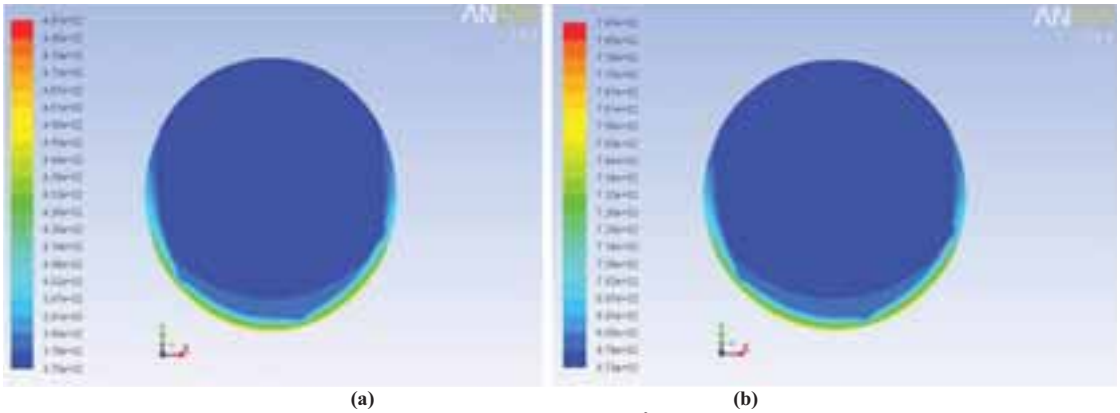

(a) (b)

Fig.7 : Temperature contours at the absorber outlet for DNI = 1000 W/m^2, V = 1 m/s for different inlet temperature (a) 100°C (b) 400°C

The non uniform radiation distribution also causes a non uniform temperature distribution. The shape of that distribution. Figure .8 shows the circumferential temperature distribution for the outer absorber surface and

the outer glass surface as function of circumferential angle around the receiver when the inlet temperature of HTF is 100˚C & 400˚C and also the DNI is 1000 W/m^2. The temperature distributions are generally smoother than the incident radiation distributions. The difference between absorber tube and HTF temperatures is significant. This is primarily due to the low heat transfer coefficient which is caused by the lower mass flow rates of HTF.

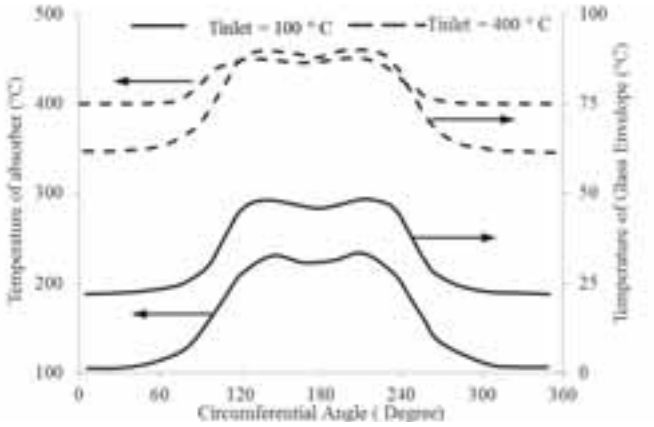

Fig. 8: Circumferential temperature distribution of absorber tube and glass envelope for Tinlet = 100˚C & Tinlet = 400˚C

For this reason, there is also a significant temperature difference between the bottom portion of the absorber surface exposed to the concentrated solar radiation and the top portion of the absorber surface which receives the direct normal irradiation from the sun. For the Tinlet = 100˚C & Tinlet = 400˚C , the difference between maximum and minimum absorber temperature is 131˚C and 55℃ respectively The convective heat transfer coefficient of HTF is increased by increasing the temperature of HTF, due to this temperature difference between the bottom and top of absorber surface and temperature difference between the HTF and absorber tube is also decreased. Similarly from the Figure , For the Tinlet = 100˚C & Tinlet = 400˚C , the difference between maximum and minimum glass envelope is 23˚C and 29 ˚C respectively. The temperature profile of both absorber and glass envelope follows the non-uniform solar heat flux distribution which indicates that the conduction in both tubes is relatively small. The temperature of the outer surface of the absorber is higher than that of the inner surface since the outer surface is the heating surface, and the maximum temperature difference is very small.

The temperature of the absorber is symmetric and increases by moving along the HCE far away from the inlet. The temperature distribution is estimated for the different inlet velocity of HTF .Fig. 9 shows the distribution of the temperature difference on the cross sectional planes of the absorber tube along the flow direction of HTF and length of the PTC receiver. The temperature difference was calculated through the difference between the maximum temperature and minimum temperature on the PTC receiver. At the entrance part of receiver, effect of temperature difference is maximum.

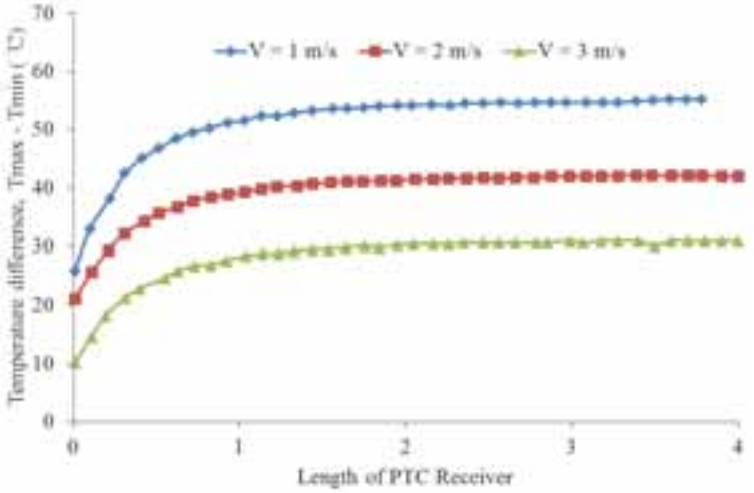

Fig. 9: Temperature distribution along the length of the PTC receiver for different inlet velocity

When the length of the receiver is within 1m, temperature difference of PTC receiver increases exponentially. Similarly when the length of receiver is greater than 1m (after the entrance region), the temperature difference almost approach constant path. This temperature difference is plotted for various HTF velocities from 1m/s to 3 m/s. However, the temperature difference decreases from 55.5˚C to 31˚C when the HTF velocity changes from 1 to 3 m/s. Therefore, the temperature differences are mainly dependent on the HTF velocity. The lower HTF velocity will cause higher temperature differences on sectional planes of the absorber tube, and this maximum temperature difference is the main cause of the breakage of PTC receiver

7. Conclusion

In this paper, three-dimensional numerical simulation of coupled heat transfer characteristics in the receiver tube is performed by combining the MCRT method and the FVM using Fluent software. Three typical testing conditions are chosen from the experiment to validate the physical model and simulation code. Numerical results show that the predicted results agree well with the experimental data, the average relative error is within 3%. The heat flux distribution on the outer surface of absorber tube was heterogeneous in circumferential direction but uniform in axial direction. Then, the coupled method was used to simulate the LS-2 Solar Collector for method verification. And the outlet temperatures of four cases were counted out and compared with Dudley et al.'s report data. The application of MC in combination with FV allowed for the incorporation of non-uniform temperature and heat transfer distributions and the identification of critical peak temperatures and heat fluxes. The temperature distributions of the absorber and the glass envelope surface are similar with the distributions of the solar energy flux. The HTF temperature difference of the cross-section decreases with the increase of the inlet velocity of the HTF, increases with the rising DNI, and almost remains the same with the increase of the inlet temperature of the HTF. Similarly when the length of receiver is greater than 1m (after the entrance region), the temperature difference almost approach constant path. This temperature difference is plotted for various HTF velocities from 1m/s to 3 m/s. However, the temperature difference decreases from 55.5˚C to 31˚C when the HTF velocity changes from 1 to 3 m/s. Therefore, the temperature differences are mainly dependent on the HTF velocity. The lower HTF velocity will cause higher temperature differences on sectional planes of the absorber tube, and this maximum temperature difference is the main cause of the breakage of PTC receiver.

Acknowledgement

The financial support provided by CSIR (Council of Scientific and Industrial Research), Government of India through the technology development project is acknowledged.

Nomenclature

C, μ	k-ε model constants
DNI	Direct Normal Irradiance (W/m^2)
g	acceleration due to gravity (m/s2)
h	heat transfer coefficient (W/m2K)
Nu	Nusselt number
P	pressure (Pa)
Ra	Rayleigh number
Re	Reynolds number
T	Temperature (K)
u,v	velocity component

Greek Symbols

λ	thermal conductivity (W/mK)
k_{in}	turbulent kinetic energy at the inlet
ρ	density (kg/m^3)
μ	dynamic viscosity (Pa.s)
μ_t	turbulent viscosity (Pa.s)
ν	kinematic viscosity (Pa.s)

Subscripts

a	absorber
f	heat transfer fluid
g	glass envelope
in	inlet
max	maximum
min	minimum
o	outlet

8. References

Chen, W., Liu, W., 2004. Numerical analysis of heat transfer in a composite wall solar collector system with a porous absorber. Appl Energy, 78, 137–49

Cheng, Z.D., He, Y. L., Cui, F.Q., Xu, R.J., Tao, Y.B., 2012. Numerical simulation of a parabolic trough solar collector with non-uniform solar flux conditions by coupling FVM and MCRT method, Sol. Energy 86, 1770–1784.

Cheng, Z.D., He, Y.L., Xiao, J., Tao, Y.B., Xu, R.J., 2010. Three-dimensional numerical study of heat transfer characteristics in the receiver tube of parabolic trough solar collector, Int. Commun. Heat Mass Transfer 37 (7), 782–787.

Clark, J., 1982. An analysis of the technical and economic performance of a parabolic trough concentrator for solar industrial process heat application. Int J Heat Mass Trans. 25(9), 427–438.

Dudley, V.E., Kolb, G.E., Mahoney, A.R., Mancini, T.R., Matthews, C.W., Sloan, M., Kearney, D., 1994. Test results: SEGS LS-2 solar collector, Report of Sandia National Laboratories, SANDIA-94-1884

Edenburn, M.W., 1976, Performance analysis of a cylindrical parabolic focusing collector and comparison with experimental results. Sol Energy 18(5), 437-444.

Fend, T., Paal, R.P., Reutter, O., Bauer, J., Hoffschmidt, B., 2004. Two novel high-porosity materials as volumetric receivers for concentrated solar radiation. Sol Energy Mater Sol Cells. 84, 291–304

Forristall R., 2003. Heat transfer analysis and modeling of a parabolic trough solar receiver implemented in engineering equation solver. National Renewable Energy Laboratory.

Güven H, Bannerot R., 1986. Derivation of universal error parameters for comprehensive optical analysis of parabolic troughs. Journal of Solar Energy Engineering, 108, 275–81.

He, Y.L., Xiao, J. Cheng, Z.D., Tao, Y.B., 2011. A MCRT and FVM coupled simulation method for energy conversion process in parabolic trough solar collector, Renewable Energy 36 (3), 976–985.

Iverson, BD., Flueckiger, SM., Ehrhart, BD., 2011. Through heat collection element deformation and solar intercept impact. SolarPACES Conference, Spain.

Kalogirou.SA., 2004. Solar thermal collectors and applications. Progress in Energy and Combustion Science 30, 231-295

KJC Operating Company, 1993. Final Report on HCE Heat Transfer Analysis Code. SANDIA Contract No. AB-0227. Albuquerque, NM: Sandia National Laboratories

Kumar, K. R., Reddy, K. S., 2009. Thermal analysis of solar parabolic trough with porous disc receiver. Appl Energy, 86, 1804–1812

Mahoney, R., 2002. Advances in parabolic trough solar power technology. J. Solar Energy Eng. 124, 109–

O'García-Valladares, Velázquez, V., 2009.Numerical simulation of parabolic trough solar collector: improvement using counter flow concentric circular heat exchangers. International Journal of Heat and Mass Transfer, 52(3), 597–609.

Padilla, R., Demirkaya, G., Goswami, Y. D., Stefanakos, E., Rahman, M., 2011. Heat transfer analysis of parabolic trough solar receiver. Applied Energy, 88(12), 5097– 5110

Pope R, Schimmel W., 1973. An analysis of linear focused collectors for solar power. In: Eighth Intersociety Energy Conversion Engineering Conference. Philadelphia, PA. 353–359.

Ratzel, A., Hickox, C., Gartling, D., 1979. Techniques for reducing thermal conduction and natural convection heat losses in annular receiver geometries. J Heat Trans, 101(1), 108–113.

Stuetzle. T., 2002. Automatic control of the 30 MWe SEGS IV Parabolic trough plant. Master's thesis, University of Wisconsin-Madison.